

Available online at [www.sciencedirect.com](http://www.sciencedirect.com)**ScienceDirect**

Energy Procedia 55 (2014) 786 – 790

---

---

**Energy**  
**Procedia**

---

---

4th International Conference on Silicon Photovoltaics, SiliconPV 2014

## Fundamental studies of hydrogen at the silicon / silicon nitride interface

Sebastian Joos<sup>a,\*</sup>, Yvonne Schiele<sup>a</sup>, Barbara Terheiden<sup>a</sup>, Hans-Werner Becker<sup>b</sup>,  
Detlef Rogalla<sup>b</sup>, Giso Hahn<sup>a</sup>

<sup>a</sup>University of Konstanz, P.O. Box 676, Department of Physics, 78457, Konstanz, Germany<sup>b</sup>Ruhr-Universität Bochum, Universitätsstr. 150, Gebäude NT 05/ 130, 44780, Bochum, Germany

---

### Abstract

The quality of the interface between silicon and a dielectric is one of the main influencing parameters for crystalline silicon surface passivation. In this work, this interface is examined by means of capacitance voltage (CV) and nuclear resonance reaction analysis (NRRA) measurements for SiN<sub>x</sub>:H as well as SiO<sub>2</sub> capped SiN<sub>x</sub>:H passivated p-type float zone silicon samples. Due to a highly sensitive NRRA measurement setup, very small differences in hydrogen concentration at the interface could be detected for the first time and a significant correlation between hydrogen concentration, interface state trap densities D<sub>it</sub> and passivation quality is found. The results of this study present easily implementable processes to improve the quality of SiN<sub>x</sub>:H surface passivation and process stability for solar cell and module production applications. First optimised industrial type Al-BSF p-type cells feature 2 mV and 0.5 mA/cm<sup>2</sup> gains in V<sub>oc</sub> and j<sub>sc</sub>, leading to efficiencies of up to 19.1%.

© 2014 The Authors. Published by Elsevier Ltd. This is an open access article under the CC BY-NC-ND license (<http://creativecommons.org/licenses/by-nc-nd/3.0/>).

Peer-review under responsibility of the scientific committee of the SiliconPV 2014 conference

**Keywords:** Passivation; silicon nitride; silicon oxide; semiconductor-insulator boundaries

---

---

\* Corresponding author. Tel.: +49-7531-88-3732; fax: +49-7531-88-3895.  
E-mail address: [sebastian.joos@uni-konstanz.de](mailto:sebastian.joos@uni-konstanz.de)

## 1. Introduction

Hydrogen is known to be a major influencing factor for silicon surface and bulk passivation. The publications of Lamers et al. [1,2] on  $\text{SiN}_x\text{:H}$  passivation indicate the interface between dielectric and silicon bulk to be the crucial location for surface passivation quality.

In this work, the  $\text{SiN}_x\text{:H}/\text{Si}$  interface is examined by means of NRRA and CV measurements. These investigations are performed on different plasma enhanced chemical vapour deposited (PECVD) dielectric layers and stacks consisting of a dense and well passivating amorphous hydrogenated  $\text{SiN}_x\text{:H}$  and a combination of this  $\text{SiN}_x\text{:H}$  and PECVD  $\text{SiO}_2$  deposited on p-type float zone silicon (FZ-Si). The determined results of hydrogen concentration at the interface (NRRA) and density of fixed charges  $Q_{\text{tot}}$  and interface state trap densities  $D_{\text{it}}$  (CV) are correlated with effective minority carrier lifetime and sample preparation.

$\text{SiN}_x\text{:H}$  is studied in this work because of its widespread usage in solar cell production. A deeper understanding of the mechanisms that lead to well passivating  $\text{SiN}_x\text{:H}$  layers is crucial for highly efficient solar cells and stable production processes.

## 2. Experimental details

For the experiments, p-type FZ-Si wafers of 2  $\Omega\text{cm}$  resistivity are used (thickness: 250  $\mu\text{m}$ ). After laser cutting and labelling, the samples are subjected to a chemical polishing/damage etch ( $\sim 5 \mu\text{m}$  each side) followed by RCA cleaning [3].  $\text{SiN}_x\text{:H}$  and  $\text{SiN}_x\text{:H}/\text{SiO}_2$  stacks are deposited on both sides of the wafers in a lab-type direct-PECVD setup (Oxford Instruments Plasmalab System 100). The process gases used for  $\text{SiN}_x\text{:H}$  are  $\text{SiH}_4$ ,  $\text{NH}_3$  and  $\text{N}_2$ , and for  $\text{SiO}_2$ ,  $\text{SiH}_4$  and  $\text{N}_2\text{O}$  are used. As there is no evidence for cross contamination between the  $\text{SiN}_x\text{:H}$  and the  $\text{SiO}_2$  deposition processes, stacked layers are deposited within one step at constant temperature. The dielectric layers and their thicknesses are depicted in Fig. 1. The thicknesses of the thin  $\text{SiN}_x\text{:H}$  layer and  $\text{SiN}_x\text{:H}/\text{SiO}_2$  layer are chosen because of their relevance as anti-reflective coatings for solar cell processing. The thick  $\text{SiN}_x\text{:H}$  layer acts as a reference layer for best passivation without solar cell production relevance. All samples are exposed to an industrial-type co-firing process step at 855°C peak set temperature in a belt furnace.

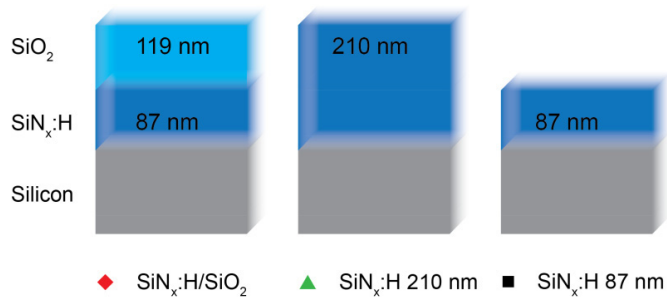


Fig. 1. Investigated dielectric layers, their respective thicknesses and the corresponding symbols for measurement data.

Effective minority charge carrier lifetimes ( $\tau_{\text{eff}}$ ) are measured via transient photoconductance decay technique by means of a WCT-120 tool from Sinton Instruments Inc. [4]. For comparability, all lifetimes are evaluated at an injection level of  $10^{15} \text{cm}^{-3}$ .

After lifetime measurement the same samples are used for NRRA and CV measurements. CV measurements have been performed at 4Dimensions Inc. using a CVmap92A measurement setup. NRRA measurements have been performed at the Central Unit for Ionbeams and Radionuclides, RUBION at the University of Bochum. Fig. 2 illustrates the simplified measurement principle [5].

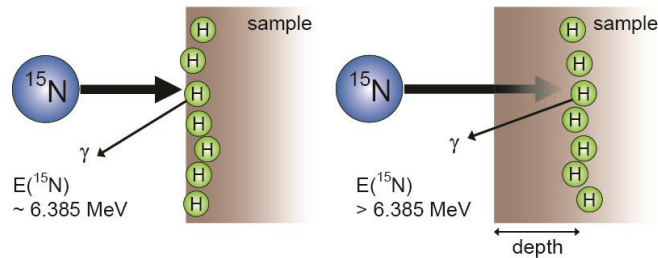


Fig. 2. Simplified NRA measurement principle. Dependent on the detected gamma quanta from a  $^{15}\text{N}$  particle beam of known kinetic energy and fluence, a [H] depth profile can be measured.

Two groups of industrial type solar cells are manufactured using  $12.5 \times 12.5 \text{ cm}^2$  boron-doped Czochralski-grown (Cz) silicon wafers ( $1.5 \Omega\text{cm}$ , thickness:  $200 \mu\text{m}$ ) featuring a  $50 \Omega/\text{sq}$   $\text{POCl}_3$  emitter and a full area Al back surface field (BSF). The front side of the cells is passivated by a  $\text{SiN}_x\text{:H}$  single layer or a  $\text{SiN}_x\text{:H/SiO}_2$  double layer antireflection coating (DARC), respectively.

### 3. Results

Table 1 displays the results from lifetime, CV and IV measurements. In this comparison, the thick  $\text{SiN}_x\text{:H}$  layer exhibits the highest lifetime value and the lowest  $D_{it}$ .

Table 1. Effective minority charge carrier lifetime, CV measurement and best solar cell results.

| Sample/dielectric              | $\tau_{eff}$ ( $\mu\text{s}$ ) | $Q_{tot}$ ( $\times 10^{12} \text{ cm}^{-2}$ ) | $D_{it}$ ( $\times 10^{10} \text{ cm}^2 \text{ eV}^{-1}$ ) | $V_{oc}$ (mV) | $j_{sc}$ ( $\text{mA}/\text{cm}^2$ ) | $\eta$ (%) |
|--------------------------------|--------------------------------|--|--|---------------|--------------------------------------|------------|
| $\text{SiN}_x\text{:H}$ 87 nm  | $722 \pm 36$                   | $2.5 \pm 0.3$                                  | leakage current  | 638           | 37.3                                 | 18.8       |
| $\text{SiN}_x\text{:H}$ 210 nm | $1365 \pm 68$                  | $2.2 \pm 0.3$                                  | $< 1 - 1.6$  | -             | -                                    | -          |
| $\text{SiN}_x\text{:H/SiO}_2$  | $1037 \pm 52$                  | $2.4 \pm 0.3$                                  | $2.1 - 3.6$  | 640           | 38.2                                 | 19.1       |

$Q_{tot}$  for all samples is approximately the same within measurement uncertainty. Therefore, a correlation to lifetime values could not be found. The  $D_{it}$  values, however, reveal dependencies as expected. The  $\text{SiN}_x\text{:H/SiO}_2$  sample exhibits a higher  $D_{it}$  value than the thick  $\text{SiN}_x\text{:H}$  sample. Due to leakage current, no  $D_{it}$  value could be calculated for the thin  $\text{SiN}_x\text{:H}$  sample, suggesting an even higher  $D_{it}$  value than found for the other samples.

A correlation of the  $\tau_{eff}$  and bond densities of Si-H and N-H in the  $\text{SiN}_x\text{:H}$  bulk was presented in our earlier work [6]. In combination with the CV results a positive effect of the capping layer in respect to the interface passivation rather than to the density of fixed charges could be stated.

At a steady FF, solar cells using the  $\text{SiN}_x\text{:H/SiO}_2$  ARC exhibit average improvements of 2 mV and  $0.5 \text{ mA}/\text{cm}^2$  in  $V_{oc}$  and  $j_{sc}$ , leading to 19.1% efficiency for the best cell.

The NRA measurements are depicted in Fig. 3. All measurements are normalized to the interface (0 MeV) and shown in relative kinetic energy of the  $^{15}\text{N}$  atoms.

The thick  $\text{SiN}_x\text{:H}$  layer sample reveals the highest concentration of hydrogen close to the interface and in the silicon bulk. The thin  $\text{SiN}_x\text{:H}$  and the  $\text{SiN}_x\text{:H/SiO}_2$  deposited samples feature comparable hydrogen concentrations in the silicon bulk. Close to the interface (0.05 MeV), however, the  $\text{SiN}_x\text{:H/SiO}_2$  sample exhibits a slightly higher hydrogen content.

The combination of the results suggest that thicker PECVD  $\text{SiN}_x\text{:H}$  layers or  $\text{SiN}_x\text{:H}$  layers capped with PECVD  $\text{SiO}_2$ , have more hydrogen available for an improved passivation or lower  $D_{it}$ , respectively. As Nickel et al. revealed,  $\text{SiO}_2$  acts as a diffusion barrier for diffusion of hydrogen into silicon [7], so this effect might be due to the slowed down effusion of hydrogen from the  $\text{SiN}_x\text{:H}$  layer to the air due to thick  $\text{SiN}_x\text{:H}$  or added  $\text{SiO}_2$ , respectively.

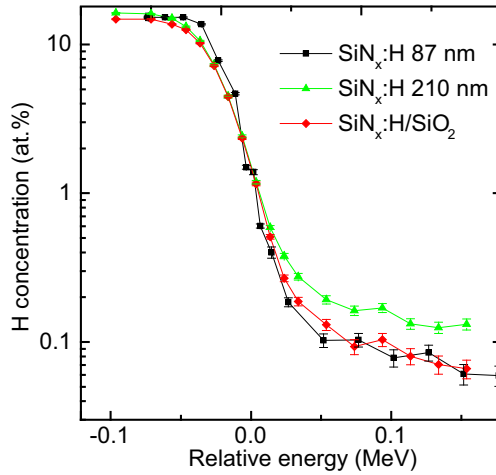


Fig. 3. NRRA measurement of hydrogen concentration after firing in the dielectric layers and silicon. x axis' zero is set to the interface between silicon and the dielectric.

Regarding solar cell production, the presented SiNx:H/SiO<sub>2</sub> double ARC is favorable not only because of its better incoupling of light and better stability against thickness variations of the depositions [8], but also due to the improved surface passivation. In contrast to combinations with a thermal oxide layer, the presented stack is the more cost effective solution. The lower leakage current of SiNx:H/SiO<sub>2</sub> compared to a thin SiNx:H layer can also be advantageous for novel solar cell concepts.

**4. Discussion about DARC on cell and module level**

To discuss the optical effect of a DARC on cell and module level numerical simulations are performed [9]. In these simulations efficiencies of cells with SiNx:H (n<sub>600 nm</sub> = 1.95) single layers (SARC) of different thicknesses alone, below 119 nm of SiO<sub>2</sub> (n<sub>600 nm</sub> = 1.48) (DARC), EVA (n<sub>600 nm</sub> = 1.53) and SiO<sub>2</sub> + EVA are investigated. The combinations without EVA represent cell level performance, whereas with EVA module level performance is represented. For the given efficiencies in Fig. 4 only optical effects are taken into account. Other cell parameters like FF, V<sub>oc</sub> and shading are treated as constants.

| SiNx thickness (nm) | η SiNx (%) | η SiNx + SiO <sub>2</sub> (%) | η SiNx below EVA (%) | η SiNx + SiO <sub>2</sub> below EVA (%) |
|---------------------|------------|-------------------------------|----------------------|---|
| 105                 | 19.78      | 20.00                         | 20.13                | 20.12                                   |
| 100                 | 19.83      | 20.02                         | 20.14                | 20.13                                   |
| 95                  | 19.88      | 20.05                         | 20.15                | 20.15                                   |
| 90                  | 19.93      | 20.08                         | 20.16                | 20.16                                   |
| 85                  | 19.97      | 20.10                         | 20.17                | 20.16                                   |
| 80                  | 19.99      | 20.13                         | 20.17                | 20.16                                   |
| 75                  | 20.00      | 20.15                         | 20.17                | 20.16                                   |
| 70                  | 19.99      | 20.17                         | 20.16                | 20.15                                   |
| 65                  | 19.96      | 20.18                         | 20.15                | 20.13                                   |
| 60                  | 19.90      | 20.18                         | 20.13                | 20.11                                   |
| 55                  | 19.82      | 20.17                         | 20.10                | 20.08                                   |
| 50                  | 19.71      | 20.16                         | 20.06                | 20.03                                   |
| 45                  | 19.57      | 20.14                         | 20.01                | 19.98                                   |
| 40                  | 19.40      | 20.11                         | 19.96                | 19.92                                   |
| 35                  | 19.20      | 20.07                         | 19.90                | 19.86                                   |
| 30                  | 19.00      | 20.03                         | 19.84                | 19.79                                   |

Fig. 4. Simulated efficiency table for different dielectric layer systems.

Fig. 4 reveals a strong dependence on the  $\text{SiN}_x\text{:H}$  layer thickness on cell level for a SARC. Within the chosen thickness range up to 1 %<sub>abs</sub> in efficiency can be lost due to not optimized layer thickness. The loss is minimized with the addition of a  $\text{SiO}_2$  capping layer. Here only 0.18 %<sub>abs</sub> is lost. Thereby the process window dramatically widens for the DARC. In addition to the improved efficiency due to a better incoupling of photons into the Si bulk for optimized layer thicknesses, deposition recipes with more inhomogeneities (e.g. process time optimized or passivation optimized) are acceptable.

On module level however this advantage diminishes. There is even a small benefit for the SARC. However, it has to be taken into account how modules are made. Cells are binned according to  $j_{sc}$  and color. For SARC there is a large gain in  $j_{sc}$  from cell to module. This could lead to problems because in the module cells with suboptimal optics are limited by cells with suboptimal electrical properties, because they are connected in series. Thereby the binning of cells gets easier for DARC cells and the binning according to color might be unnecessary, because the color impression of DARC cells in modules is more homogeneous as well [7]. Taking the improved  $V_{oc}$  into account the temperature coefficient of the module can be slightly improved, leading to a minor efficiency gain with a simplification of the module production process.

## 5. Conclusion

The hydrogen content close to the silicon/dielectric interface is found to be a good measure for passivation quality of  $\text{SiN}_x\text{:H}$  coated silicon samples. With thicker  $\text{SiN}_x\text{:H}$  layers or the addition of a  $\text{SiO}_2$  capping layer, the hydrogen content at the interface can be increased and thereby the passivation quality improved. With advantages in surface passivation, optics, cost and process stability the presented PECVD stack made of  $\text{SiN}_x\text{:H}/\text{SiO}_2$  is favorable for efficient solar cell and module production.

## Acknowledgements

Part of this work was supported by the German Federal Ministry for the Environment, Nature Conservation and Nuclear Safety.

## References

- [1] Lamers M et al. The interface of a- $\text{SiN}_x\text{:H}$  and Si: Linking the nano-scale structure to passivation quality. *Sol En Mat and Sol Cells* 2014;311-6.
- [2] Lamers MWPE, Butler KT, Harding JH, Weeber A. Interface properties of a- $\text{SiN}_x\text{:H}/\text{Si}$  to improve surface passivation. *Sol En Mat and Sol Cells* 2012;106:17–21.
- [3] Reinhardt KA, Kern W. Handbook of silicon wafer cleaning technology. Norwich: William Andrew Publishing; 2008.
- [4] Sinton RA, Cuevas A, Stuckings M. Quasi-steady-state photoconductance, a new method for solar cell material and device characterization. In *Proc 25<sup>th</sup> IEEE PVSC*; 1996. p. 457-60.
- [5] Schatz G, Weidinger A. Nukleare Festkörperphysik. Stuttgart: B.G. Teubner; 1997.
- [6] Joos S, Wilking S, Schiele Y, Herguth A, Hess U, Seren S, Terheiden B, Hahn G. Hydrogen in stacked dielectric Layers. In: *Proc 28<sup>th</sup> EUPVSEC*; 2013. p. 1113–6.
- [7] Nickel NH, Jackson WB, Wu IW, Tsai CC, Chiang A. Hydrogen permeation through thin silicon oxide films. *Phys Rev B* 1995;52(11):7791-5.
- [8] Junghaenel M, Schädel M, Stolze L, Peters S. Black multicrystalline solar modules using novel multilayer antireflectance stacks. In: *Proc 25<sup>th</sup> EUPVSEC*; 2010. p. 2637-41.
- [9] Excel sheet developed by students in the webinar Advanced silicon photovoltaics by Altermatt PP, Leibniz University of Hannover, Germany. The calculations are based on Macleod HA. *Thin-Film Optical Filters*. Boca Raton: CRC Press; 2010. and on Baker-Finch SC, McIntosh KR. Reflection of normally incident light from silicon solar cells with pyramidal texture. *Progr Photovolt Res Appl* 2011;19:406-16.